Tomography of DNA Tiles Influences the Kinetics of Surface-Mediated DNA Self-Assembly

Cuizheng Zhang, Victoria E. Paluzzi, Chengde Mao*

¹Department of Chemistry, Purdue University, West Lafayette, IN 47907

mao@purdue.edu

Abstract

This manuscript studies the impact of extruding hairpins on two-dimensional self-assembly of DNA tiles on solid surface. Hairpins are commonly used as tomographic markers in DNA nanostructures for atomic force microscopy (AFM) imaging. In this study, we have discovered that hairpins play a more active role. They modulate the adsorption of the DNA tiles onto the solid surface, thus, change the tile assembly kinetics on the solid surface. Based on this discovery, we were able to promote or slow down the DNA self-assembly on surface by changing the hairpin locations on the DNA tiles. This knowledge gained will be helpful for the future design of DNA self-assembly on surface.

Statement of Significance

Extruding elements on DNA tiles are convenient tomographic markers to allow for the visualization of the tile arrangement in large architectures. At the same time, such elements make the DNA tiles bumpy. In this study, we have found that (1) the bumpiness will decrease the adsorption of the DNA tiles onto the surface and (2) this will directly attenuate the sticky-end cohesion between tiles if the extruding elements are too close to the sticky ends. This lesson learned will help us to design DNA nanostructures with extruding parts more rationally to achieve the desired structures.

Introduction

Hairpin structures are commonly used in DNA self-assembly as tomographic markers/reporters under atomic force microscopy (AFM) imaging. (1,2) They extrude from flat DNA structures and can be clearly visualized by AFM because they are taller than surrounding DNA planes. Their distribution in AFM images allows people to confidently examine whether the designed structures formed or not. (3-8) It is assumed, though not explicitly stated, that hairpins do not influence the assembly of DNA nanostructures, particularly, two-dimensional (2D) crystals. The assumption generally is true for DNA self-assembly in solution. However, in recent years, surface-mediated DNA self-assembly has drawn more attention due to the advantages it offers over solution assembly in aspects including assembling large-size and complex DNA nanostructure and avoiding sample transfer from solution to surface. (9-13) Will hairpins influence the DNA self-assembly on surface? It is an open, but urgent question to the field.

Taking the double-crossover (DX) structure as a model system, we systematically studies how the hairpin positions on a DX tile could influence the assembly rate of DNA tiles on the mica surface by a geometric effect. We conclude that, to achieve high self-assembly efficiency, hairpins should be placed in the middle of the tiles and away from the sticky ends.

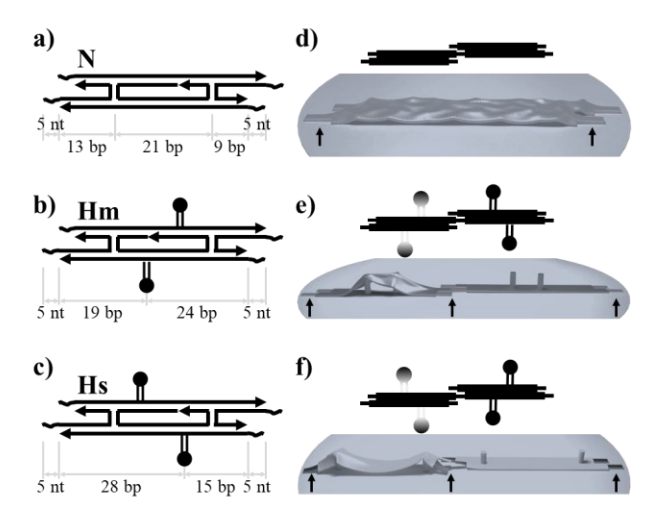


Figure 1. Geometric impact of hairpin locations on the surface-mediated self-assembly of DAE-O tiles. (a-c) The designs of three symmetric DX tiles **N** (no-hairpin), **Hm** (hairpin in the middle), and **Hs** (hairpin on the sides). They have the same pair of 5-nt (nucleotide) long sticky ends. The arrows indicate 3' ends. Schemes of tiles (d) **N**, (e) **Hm**, or (f) **Hs** adsorbed onto the mica surface with alternatingly facing up and down. The black arrows point on the sticky ends.

This study investigated surface-mediated self-assembly of 2D arrays of symmetric DX motifs. The first type of molecules is a series of DAE-O tiles containing an in-plane, two-fold rotational symmetry (Figure 1). In a DAE-O tile, the continuous strands on the two component duplexes run in antiparallel orientation and the two crossover points are separated by an even number of half turns (2 turns or 21 base pairs, bps, to be specific). (14) When two DAE-O tiles associate with each other, the two adjacent crossover points from two tiles are separated from each other by an odd number of half turns (2.5 turns or 27 bps here), thus any two associating tiles will face in opposite directions. One tile has no-hairpin (N), the other two tiles have hairpins either in the middle (Hm) or on the sides (Hs). Tile N, without hairpins, is flat, thus, can readily adsorb onto the mica surface to associate with each other into 2D arrays (Figs. 1a and 1d). However, tiles **Hm** and **Hs** each have a pair of hairpins extruding out from the tile plane. When they are adsorbed onto the mica surface and associating into 2D arrays, the hairpins in one tile will point away from the surface and the hairpins in the tiles next to it will be buried underneath the tile plane (Fig. S1). Due to this non-planar feature, both tiles **Hm** and **Hs** cannot fully adsorb onto the mica surface, thus, have difficulty to self-assemble on the surface. For tile Hs, the hairpins are close to the side of the tile, 28 bps from one sticky end and 15 pbs from the other. The buried hairpin will seriously prevent the near sticky end from attaching to the mica surface and further prevent effective sticky-end cohesions; thus, the self-assembly will be quite slow (Figs. 1c and 1f). Tile **Hm** will have the same problem, but to a lesser extent. In tile **Hm**, the hairpins are almost in the middle of the tile, 19 bps away from one sticky end and 24 bps away

from the other. Thus, the buried hairpins are away from the sticky ends and causes less disturbance to the sticky-end cohesions on the mica surface (Figs. 1b and 1e).

Materials and Methods

Oligonucleotides

All DNA strands were purchased from IDT, Inc. and purified by denaturing PAGE, and their concentrations were quantified by UV-Vis spectroscopy at 260 nm.

DNA sequences:

1A: 5'-GCAAGTAGGAGTCACCATTCCGCAAGTAGGAGTCACCATTCC-3'

1B: 5'-GGAGTCACCATAGGTAGGAGCGGAGTCACCATAGGTAGGAGC-3'

2A: 5'-AGCTGGCTAAGACCTGACTCCTACTTGCGGAATGGACATGACACGACG-3'

2B: 5'-AGCTGGCTAAGACCTGACTCCGCTCCTACGTGGCTTTTTGCCACTTCTATGG ACATGACACGACG-3'

2C: 5'-AGCTGGCTAAGACCTGACTCGGACGTTTTCGTCCTTCTACTTGCGGAATGG ACATGACACGACG-3'

3A: 5'-CAGCTCGTCGTGTCATGTGGTCTTAGC-3'

M0: 5'-CCTCAACGCTAGTGGTACTACACAGATGGACTCACCTATCCG-3'

T0: 5'-CGAAGAGGACTAGCCTGGCTTTTGCCAGTTGTTGAGGCGGATAGGACGAC AGCGGACA-3'

B0: 5'-CCGAGACCTGAGTCGGAGCTTTTGCTCCTTCATCTGTGTAGTACCTGAGAA CGTGTCC-3'

L0: 5'-CGTTCTCACCTCTTCGGCACT-3'

R0: 5'-GCTGTCGTGGTCTCGGAGTGC-3'

Tiles:

N: 1A + 2A + 3A (1:2:2)

Hm: 1B + 2B + 3A (1:2:2)

Hs: 1A + 2C + 3A (1:2:2)

E: M0 + T0 + B0 + L0 + R0 (1:1:1:1:1)

Buffers:

TAE/Mg²⁺ buffer: 40 mM tris base, 20 mM acetic acid, 2 mM EDTA, and 12.5 mM magnesium acetate; pH is adjusted to 8.0.

TA/Mg²⁺/Ni²⁺ buffer: 40 mM tris base, 20 mM acetic acid, 10 mM magnesium acetate and 2 mM nickel chloride; pH is adjusted to 8.0.

Native polyacrylamide gel electrophoresis (PAGE)

10% polyacrylamide (acrylamide/bisacrylamide at 19:1, 5% crosslinking), was electrophoresed in TAE/Mg²⁺ buffer on a FB-VE10-1 electrophoresis unit (FisherBiotech) at room temperature (150V, constant voltage). After electrophoresis, the gels were stained with Stains-all dye (Sigma) and scanned.

Assembly of DNA 2D arrays through surface slow anneal

Selected DNA strands at designated concentrations were mixed in 400 μ L TAE/Mg²⁺ buffer with a freshly cleaved mica disc and annealed slowly from 95 °C to 22 °C over 60 hours.

AFM imaging

All the samples were scanned on the Bruker Multimode 8 AFM at SCANASYST-FLUID mode with ScanAsyst-fluid+ probe (Bruker). After assembly of DNA 2D arrays through surface slow anneal, the mica disc was taken out of the assembly solution and washed 3 times with 30 μ L TAE/Mg²+ buffer. 30 μ L TAE/Mg²+ buffer was then added onto the mica surface before imaging in fluid mode. FFT (fast Fourier transform) and inverse FFT were was performed by Spectrum 2D function, and the tile height was analyzed by Section function by using the software Nanoscope Analysis 1.5 (Bruker).

The kinetics study of the growth rate of different tiles

Selected DNA strands at designated concentrations were mixed in 400 μ L TAE/Mg²⁺ buffer. Sequentially regularly annealed the solution: 95 °C for 5 min, 65 °C for 30 min, 50 °C for 30 min, 37 °C for 30 min, and 22 °C for 30 min. After that, added 30 μ L forementioned solution onto a freshly cleaved mica surface and incubated for designated time, then gently removed the solution and washed once with 30 μ L TAE/Mg²⁺ buffer gently pipetted off the solution on the surface; after that, added 30 μ L TAE/Mg²⁺ buffer and gently pipetted the buffer off again. 30 μ L TA/Mg²⁺/Ni²⁺ buffer was added onto the mica surface before imaging in fluid mode. The detailed method to measure the DNA coverage in an AFM image is in the end of the Supplemental Information.

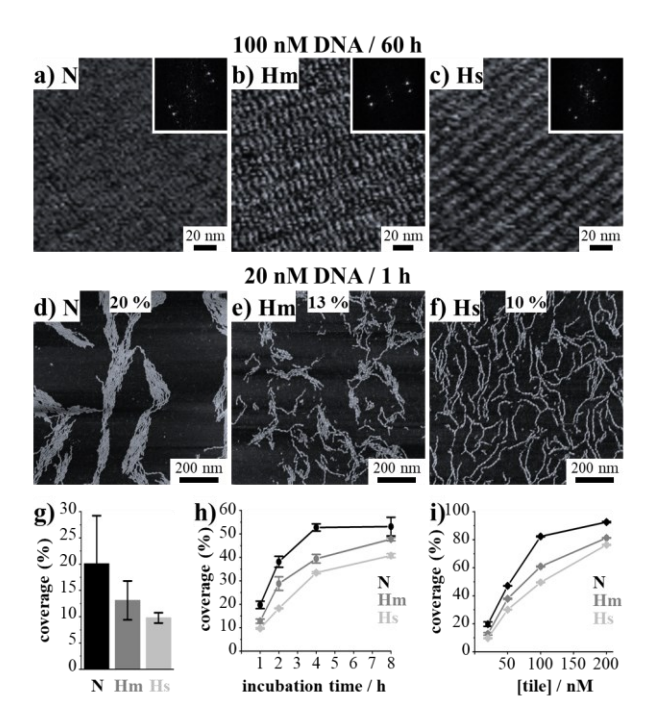


Figure 2. AFM imaging study of the impact of hairpins on surface-mediated self-assembly. Complete DNA arrays assembled from tiles (a) N, (b) Hm, and (c) Hs. Insets show corresponding FFT patterns. Incomplete DNA assembly from regular anneal tiles (d) N, (e) Hm, and (f) Hs. The surface DNA coverage is indicated in the top middle of each image. (g) Variation of DNA coverage over the AFM image fields (d-f). The black lines represent the standard deviations (n = 9). The surface DNA coverage as a function (n=4) of (h) incubation time at 20 nM DNA concentration and (i) DNA tile concentration with 1 hr incubation. The short, vertical lines represent the standard deviations.

Results and Discussion

Experimental studies have confirmed the self-assembly behaviors and kinetics of 2D DNA arrays could be controlled based on the position of the hairpins, even though they have exactly the same pair of 5-nt long sticky ends (Figure 2). Individual tiles readily formed (Figs. S2-S4) and self-assembled into homogenous, periodic 2D arrays on the mica surface via slow anneal from 95 °C to 22 °C over 60 hours (Figs. 2a-2c). The regularity of the arrays was evidenced by the fast Fourier transform (FFT) patterns. The periodicity was consistent between the measured values [16.7, 16.8, and 16.2 nm for arrays assembled from tiles **N** (Fig. 2a), **Hm** (Fig. 2b), and **Hs** (Fig. 2c), respectively] and the value (15.5 nm) calculated from the design, assuming 0.34 nm/bp (15).

When changing the self-assembly condition far away from the thermal dynamic equilibrium state, such as using lower DNA concentration and shorter assembly time, the difference in the self-assembly kinetics became obvious. When incubating 20 nM of tiles on a freshly cleaved mica surface for one hour, tile **N** had the highest surface coverage (20 %) and almost all of the **N** tiles formed 2D arrays (Fig. 2d). For tile **Hm**, the surface coverage decreased to 13 % and only some of the **Hm** tiles formed 2D arrays while others formed 1D fibers (Fig. 2e). But for the tile **Hs**, only 1D fibers were formed with the least surface coverage, 10 % (Fig. 2f). 1D fibers might come from mismatches between the sticky ends to avoid the flipping nature of intact 2D arrays at

the cost of the association energy between complementary sticky ends and the stacking energy of continuous B-type DNA duplexes (Fig. S5). (16)

To quantitatively distinguish among intact 2D arrays, partial 2D arrays / partial 1D fibers, and 1D fibers, the variation of the surface coverage across different regions of the AFM images were compared (Fig. 2g). Three forementioned AFM images at unequilibrated kinetical state were divided into nine, equal-sized sections (Figs. S6, S9, and S12). In some sections of Figure S6, the N tiles formed 2D arrays with nearly 100 % surface coverage, meanwhile, other sections might be empty with nearly 0 % surface coverage. Thus, the tile N array had the highest standard deviation, 9.2 %, under these conditions. But for the 1D fibers of tile Hs, the surface coverage was uniform in all nine sections (Fig. S12) with the lowest standard deviation, 1.0 %. In contrast, tile Hm had a modest surface coverage variance, 3.7 % (Fig. S9), which reflected the added influence of the 2D arrays and the 1D fibers.

The kinetics research of different incubation time and tile concentration was also tested. When incubating 20 nM of tiles for longer time, tile N always had the highest surface coverage compared with tiles Hm and Hs (Fig. 2h) and reached a plateau after four hours (Fig. S7). In contrast, the surface coverage for both tiles Hm and Hs continuously increased in the first eight hours and tile Hs always had the lowest surface coverage with a lot of 1D fibers (Fig. S13). When increasing the tile concentration but keeping the incubation time to one hour, all of them formed 2D lattice domains rather than 1D fibers (Figs. S8, S11, and S14) because the 2D arrays were the energy-favorable products. As well, the overall surface coverage tendency (tiles N > Hm > Hs) was still maintained (Fig. 2i), which further confirmed the influence of the hairpin position on the self-assembly behaviors and kinetics.

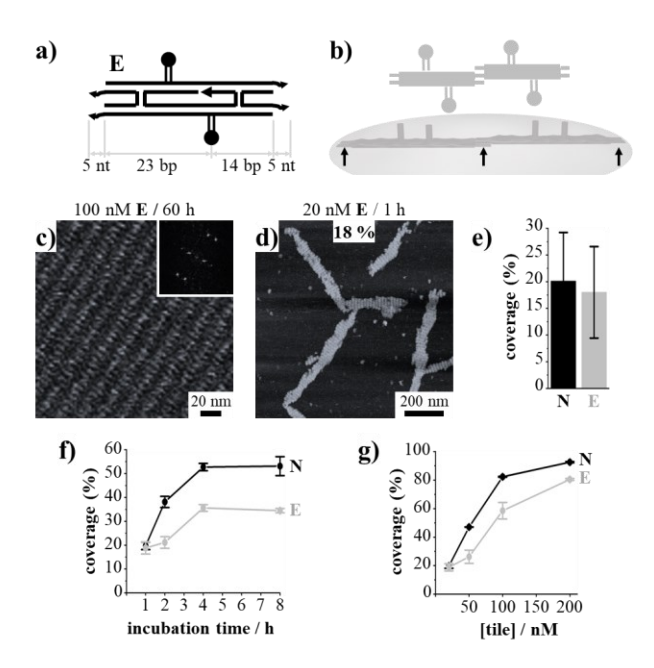


Figure 3. Kinetics-controlled self-assembly of 2D DNA array from a DAE-E molecule (tile **E**). (a) The design of tile **E**. (b) Adsorption and association of tile **E** on the mica surface without alternatingly flipping. The black arrows point on the sticky ends. AFM images of (c) complete and (d) incomplete surface-mediated DNA assembly. (e) Variation of DNA coverage over the

AFM image fields (n = 9). The surface DNA coverage as a function (n=4) of (h) incubation time at 20 nM DNA concentration and (i) DNA tile concentration with 1 hr incubation.

To confirm the hairpin impact, we designed a DAE-E molecule without an in-plane two-fold rotational symmetry (Figures 3 and S15). With this design, when any two tiles associate with each other, the distance between two crossover points from the two interacting tiles is an even number of half-turns (4 half-turns or 21 bps here). Thus, all E tiles in an assembled 2D array will face to the same side instead of facing up and down alternatingly (Figs. 3a and 3b). In this arrangement, the DNA tile could effectively adsorb onto the mica surface with its flat surface facing down to contact the mica surface and leave the hairpins facing in solution. The tiles can readily self-assemble into homogenous, periodic 2D arrays with a 14.5 nm repeating distance (13.6 nm from the design) by slow anneal from 95 °C to 22 °C over 60 hours (Fig. 3c). Incubating 20 nM of tile E on a freshly cleaved mica surface for one hour resulted in a surface coverage of 18 % (Fig. 3d), which was comparable to that of tile N. At the same time, the standard deviation of the DNA coverage on the surface, under AFM imaging, was high, 8.6 % (Figs. 3e and S16). The self-assembly of tile E reached a plateau after four hours of incubation (Figs. 3f and S17), although the surface coverage at all tested conditions was smaller than that of tile N (Figs. 3g and S18). This might come from the self-correction of the hairpin orientation. All these behaviors cross-validated that the abnormal self-assembly behaviors and kinetics of tiles Hm and Hs came from the flipping nature of DAE-O molecules and the position of hairpins in the tiles.

Conclusion

In summary, we have discovered that the extruding elements (e.g., hairpins) and their locations relative to the sticky ends have a fundamental influence on surface-mediated DNA self-assembly. This property could be used to control the DNA self-assembly behaviors and kinetics of forming 2D DNA arrays. This study reminds us that extruding elements [including hairpins, single-strands (17-20), or post-modifications of polymers (21,22), nanoparticles (23,24), etc.] hairpins, and potentially other extruding elements [including single-strands (17-20), or post-modifications of polymers (21,22), nanoparticles (23,24), etc.] as well, should be considered more carefully in designing DNA nanostructures to achieve both thermodynamically and kinetically favorable products.

Author Contributions

C.Z.Z., designed and conducted research, analyzed data, wrote and reviewed the manuscript; V.E.P., conducted research, wrote and reviewed the manuscript; C.D.M., supervised the project, analyzed data, wrote and reviewed the manuscript.

Declaration of Interests

The authors declare no competing financial interest.

Acknowledgements

We would like to devote this article to Prof. Nadrian Seeman, a pioneer, a mentor, and a dear friend. This work was financially supported by NSF (CCF-2107393 and CCMI-2025187 to C.M.).

References

- 1. Winfree, E., F. Liu, L. A. Wenzler, and N. C. Seeman. 1998. Design and self-assembly of two-dimensional DNA crystals. *Nature* 394:539-544.
- 2. Rothemund, P. W. 2006. Folding DNA to create nanoscale shapes and patterns. *Nature* 440:297-302.
- 3. Rothemund, P. W., N. Papadakis, and E. Winfree. 2004. Algorithmic self-assembly of DNA Sierpinski triangles. *PLoS Biol* 2:e424.
- 4. Schulman, R., C. Wright, and E. Winfree. 2015. Increasing Redundancy Exponentially Reduces Error Rates during Algorithmic Self-Assembly. *ACS Nano* 9:5760-5771.
- 5. Liu, F., R. Sha, and N. C. Seeman. 1999. Modifying the Surface Features of Two-Dimensional DNA Crystals. *J. Am. Chem. Soc.* 121:917-922.
- 6. Cho, H., S. B. Mitta, Y. Song, J. Son, S. Park, T. H. Ha, and S. H. Park. 2018. 3-Input/1-Output Logic Implementation Demonstrated by DNA Algorithmic Self-Assembly. *ACS Nano* 12:4369-4377.
- 7. Tandon, A., Y. Song, S. B. Mitta, S. Yoo, S. Park, S. Lee, M. T. Raza, T. H. Ha, and S. H. Park. 2020. Demonstration of Arithmetic Calculations by DNA Tile-Based Algorithmic Self-Assembly. *ACS Nano* 14:5260-5267.
- 8. Zhang, C., M. Zheng, Y. P. Ohayon, S. Vecchioni, R. Sha, N. C. Seeman, N. Jonoska, and C. Mao. 2022. Programming DNA Self-Assembly by Geometry. *J Am Chem Soc* 144:8741-8745.
- 9. Sun, X., S. Hyeon Ko, C. Zhang, A. E. Ribbe, and C. Mao. 2009. Surface-mediated DNA self-assembly. *J Am Chem Soc* 131:13248-13249.
- 10. Hamada, S., and S. Murata. 2009. Substrate-assisted assembly of interconnected single-duplex DNA nanostructures. *Angew Chem Int Ed Engl* 48:6820-6823.
- 11. Li, Z., M. Liu, L. Wang, J. Nangreave, H. Yan, and Y. Liu. 2010. Molecular behavior of DNA origami in higher-order self-assembly. *J Am Chem Soc* 132:13545-13552.
- 12. Aghebat Rafat, A., T. Pirzer, M. B. Scheible, A. Kostina, and F. C. Simmel. 2014. Surface-assisted large-scale ordering of DNA origami tiles. *Angew Chem Int Ed Engl* 53:7665-7668.
- 13. Avakyan, N., J. W. Conway, and H. F. Sleiman. 2017. Long-Range Ordering of Blunt-Ended DNA Tiles on Supported Lipid Bilayers. *J Am Chem Soc* 139:12027-12034.
- 14. Fu, T.-J., and N. C. Seeman. 1993. DNA double-crossover molecules. *Biochemistry* 32:3211-3220.
- 15. Wang, J. C. 1979. Helical repeat of DNA in solution. *Proc Natl Acad Sci U S A* 76:200-203.
- 16. Yakovchuk, P., E. Protozanova, and M. D. Frank-Kamenetskii. 2006. Base-stacking and base-pairing contributions into thermal stability of the DNA double helix. *Nucleic Acids Res.* 34:564-574.
- 17. Ke, Y., S. Lindsay, Y. Chang, Y. Liu, and H. Yan. 2008. Self-assembled water-soluble nucleic acid probe tiles for label-free RNA hybridization assays. *Science* 319:180-183.
- 18. Gu, H., J. Chao, S. J. Xiao, and N. C. Seeman. 2010. A proximity-based programmable DNA nanoscale assembly line. *Nature* 465:202-205.
- 19. Lund, K., A. J. Manzo, N. Dabby, N. Michelotti, A. Johnson-Buck, J. Nangreave, S. Taylor, R. Pei, M. N. Stojanovic, N. G. Walter, et al. 2010. Molecular robots guided by prescriptive landscapes. *Nature* 465:206-210.
- 20. Chao, J., J. Wang, F. Wang, X. Ouyang, E. Kopperger, H. Liu, Q. Li, J. Shi, L. Wang, J. Hu, et al. 2019. Solving mazes with single-molecule DNA navigators. *Nat Mater* 18:273-279.

- 21. Knudsen, J. B., L. Liu, A. L. Bank Kodal, M. Madsen, Q. Li, J. Song, J. B. Woehrstein, S. F. Wickham, M. T. Strauss, F. Schueder, et al. 2015. Routing of individual polymers in designed patterns. *Nat Nanotechnol* 10:892-898.
- Tokura, Y., Y. Jiang, A. Welle, M. H. Stenzel, K. M. Krzemien, J. Michaelis, R. Berger, C. Barner-Kowollik, Y. Wu, and T. Weil. 2016. Bottom-Up Fabrication of Nanopatterned Polymers on DNA Origami by In Situ Atom-Transfer Radical Polymerization. *Angew Chem Int Ed Engl* 55:5692-5697.
- 23. Yan, H., S. H. Park, G. Finkelstein, J. H. Reif, and T. H. LaBean. 2003. DNA-templated self-assembly of protein arrays and highly conductive nanowires. *Science* 301:1882-1884.
- 24. Ding, B., Z. Deng, H. Yan, S. Cabrini, R. N. Zuckermann, and J. Bokor. 2010. Gold nanoparticle self-similar chain structure organized by DNA origami. *J Am Chem Soc* 132:3248-3249.